行政院國家科學委員會專題研究計畫成果報告

※※※※※※※※※※※※※※※※※※※※※※※※※※※※※※※※※※※※※※
※ ※
※ 有限域孔隙介質底床受水波或地震波引發土壤液化之解析 ※
※ **Study on soil liquefaction due to water wave or earthquake wave** ※
※ **in finite thick porous material bed** ※
※ ※
※※※※※※※※※※※※※※※※※※※※※※※※※※※※※※※※※※※※※※

計畫編號： NSC 89 — 2611 — E002 — 051

執行期間： 89 年 8 月 1 日至 90 年 7 月 31 日

計畫主持人： 黃 良 雄

研究生助理：

處理方式：□可立即對外提供參考
（請打∨）☑一年後可對外提供參考
□（必要時，本會得展延發表時限）

執行單位：國立台灣大學水工試驗所

中華民國 90 年 7 月 日

行政院國家科學委員會專題研究計畫成果報告

有限域孔隙介質底床受水波或地震波引發土壤液化之解析
Study on soil liquefaction due to water wave or earthquake wave in finite thick porous material bed

計畫編號：NSC 89-2611-E-002-051
執行期限：89 年 8 月 1 日至 90 年 7 月 31 日
主持人：黃良雄教授　國立臺灣大學土木工程學系

Abstract

This study investigates the dynamic response of soft porous bed of finite thickness under the effect of periodically nonlinear water wave. The wave and homogeneous water are processed by potential theory and the porous material is treated by Biot's poroelastic theory herein. The analytical solutions are obtained by boundary layer correction approach combined with two-parameter perturbation expansion. The results are compared with those of soft porous bed of semi-infinite thickness to show the impermeable rigid boundary effects.

Keywords : boundary layer correction; two-parameter perturbation expansion; boundary effect

摘要

本研究係探討有限域軟孔隙彈性介質底床受週期性的非線性水波作用時之動力反應，文中採用勢流理論處理非線性水波及均質水體，以 Biot 孔隙彈性介質理論處理透水孔隙底床。解析的方法係以邊界層修正法配合雙參數微擾展開方式求解，並與半無限域透水孔隙底床之解析結果進行比較，以明瞭軟孔隙彈性介質底床受不透水剛性邊界效應影響之情形。

關鍵詞：邊界層修正法、雙參數微擾展開、邊界效應

一、前言

水與沙互動之力學機制極為複雜，若將泥沙視為彈性固體，則包含水、沙二者之孔隙介質可引用 Biot (1956)之孔隙彈性介質理論描述其運動行為之物理機制。由波場所衍生於底床質中的孔隙壓力和有效應力，若因為剪力破壞或土壤液化，將可能導致底床的不穩定，並且此種底床不穩定的土壤液化現象，將會危害許多海岸工程結構物的安全。

關於非線性水波的探討，Mei (1983)、Fenton (1985)及 Dean and Dalrymple (1991)均利用著名的史脫克展開式(Stokes expansion)，處理不透水剛性底床的深水波非線性問題，即以波幅比波長的一微小參數 k_0a，進行微擾法展開。然而它的缺點除了如傳統的史脫克展開法在波幅比波長的參數 k_0a 第三階以上會出現永久項(secular term)，使問題必須對波頻加以修正，變得異常複雜外，另外針對海洋問題上不討論底床的變形和透水特性等，也是不夠完善之處。此外，Chen et al. (1997) 亦採用史脫

克展開式展開至第二階，以微擾法解析非線性水波作用下，平坦孔隙彈性介質透水底床之動力反應，發現史脫克展開式即使在 Ursell 參數很小時，僅適用於剛性底床而不適用於軟性底床，其原因在於孔隙介質內存在有邊界層之影響，此觀點與 Liu and Dalrymple（1984）最早考慮孔隙介質內邊界層效應之研究相同。Liu and Dalrymple（1984）係採用 Dagan (1979) 所提出之廣義 Darcy 定律模式，以邊界層 Poincaré 法推估水波因底床透水之遞減率。

最近黃良雄（1998）和謝平城（1999）的研究利用勢流理論處理水波，以邊界層修正法處理孔隙彈性介質以解析非線性水波作用在半無限域軟孔隙彈性介質底床下之動力反應並修正Huang and Song (1993) 之線性解。基於透水底床常為有限厚度的事實，因而本研究沿用邊界層修正法配合雙參數微擾展開方式，進一步探討有限域軟孔隙彈性介質底床受非線性水波作用時（見圖 1）之動力反應，並與半無限域底床之結果做一比較。

二、邊界值問題之建立

假設區域(1)中水體為無黏滯性且不可壓縮，以及水流為非旋性流場，則可將連續方程式及動量方程式化為 Laplace 方程式和 Bernoulli 方程式。而將孔隙介質底床視為孔隙彈性體，其動力特性可以 Biot 所建立之孔隙彈性介質理論加以描述，即其固體結構之運動滿足線彈性理論，而介質中流體與固體結構間之摩擦力與其彼此平均運動之相對速度成正比，即流體運動滿足 Darcy 定律。另由固體與流體之連續方程式配合流體之狀態方程式，考慮孔隙間流體之微可壓縮性，對孔隙率進行微擾展開，並予線性化後可得瀦蓄方程式（storage equation）如下（見 Verruijt, 1969）：

$$\frac{\partial p^{*(2)}}{\partial t^*} = -\frac{K}{n_0}\left[(1-n_0)\nabla\cdot\left(\frac{\partial d^*}{\partial t^*}\right)+n_0\nabla\cdot\left(\frac{\partial D^*}{\partial t^*}\right)\right], \qquad (1)$$

式中，$p^{*(2)}$ 為擾動孔隙水壓力，K 為流體之容積彈性模數，n_0 為孔隙介質之孔隙率。

參考 Huang and Chwang (1990)，引入兩個純量位勢 (scalar potential) $\Phi_1^{*(2)}$ 和 $\Phi_2^{*(2)}$，及一個向量位勢 (vector potential) $\Phi_3^{(2)}e_z$，分別表示兩種膨脹波及一種旋轉波，可進而將固體與流體之位移向量表示為

$$d^* = \nabla\Phi_1^{*(2)} + \nabla\Phi_2^{*(2)} + \nabla\times\Phi_3^{(2)}e_z, \qquad (2)$$

$$D^* = \alpha_1\nabla\Phi_1^{*(2)} + \alpha_2\nabla\Phi_2^{*(2)} + \alpha_3\nabla\times\Phi_3^{(2)}e_z. \qquad (3)$$

其中，α_1、α_2、α_3 分別為各種波所造成之流體位移與固體位移間之比例係數，e_z 為垂直 xy 平面之單位向量。除去時間因子 $e^{-i\Omega t}$ 後，並進一步化簡後可得到三條不偶合(decoupled)之 Helmholtz 方程式：

$$\nabla^2\Phi_j^{(2)} + k_j^2\Phi_j^{(2)} = 0, \ \text{j=1,2,3.} \qquad (4)$$

式中，k_1、k_2、k_3 分別是第一種、第二種膨脹波及旋轉波之波數(wave number)，均與波動頻率及底床材料特性有關。

至於本問題之邊界條件則分別在：一、自由水面($y=h+\eta^*$)，包括運動邊界條件和動力邊界條件；二、水流與底床交界面（$y=\xi^*$），包括擾動壓力連續條件、流體通量連續條件和有效應力連續條件；及三、不透水底床($y=-B$)，包括無位移發生和無流體通量。最後將邊界條件於 $y=\xi^*$ 及 $y=h+\eta^*$ 處，分別對 ξ^* 及 η^* 做泰勒級數展開（Taylor series expansion）而分別移轉至 $y=0$ 及 $y=h$ 處，即邊界條件以 $\sum_{m=0}^{\infty}\frac{(\eta^*)^m}{m!}\frac{\partial^m}{\partial y^m}$ 和 $\sum_{m=0}^{\infty}\frac{(\xi^*)^m}{m!}\frac{\partial^m}{\partial y^m}$ 修改之。

由於在軟孔隙彈性介質底床部份之控制方程式，各項間量階存在有差異很大之情形，故將原邊界值問題中之各物理量經由量階分析後，找出無因次化之表示式如次：$\hat{x}=k_0x$，$\hat{y}=k_0y$，$y'=\hat{y}/\varepsilon_2$ (僅使用於第二種膨脹波之垂直方向長度尺度)，$\hat{t}=\sqrt{gk_0}t$，$\hat{\eta}^*=k_0\eta^*$，$\hat{\omega}=\omega/\sqrt{gk_0}$，$\hat{\Phi}^{*(1)}=\frac{k_0^2}{\sqrt{gk_0}}\Phi^{*(1)}$，

$$\hat{\Phi}_1^{*(2)}=e^{k_0h}k_0^2\Phi_1^{*(2)},\quad \hat{\Phi}_2^{*(2)}=\frac{e^{k_0h}k_0^2}{\varepsilon_2^2A^2}\Phi_2^{*(2)},$$

$$\hat{\Phi}_3^{*(2)} = e^{k_0 h} k_0^{\,2} \Phi_3^{*(2)}, \quad \hat{\xi}^* = \frac{k_0 e^{k_0 h}}{\Psi^2} \xi^*,$$

$$\hat{P}^{*(1)} = \frac{k_0}{\rho_0 g} P^{*(1)}, \quad \hat{P}^{*(2)} = \frac{k_0}{\rho_0 g} P^{*(2)}. \qquad (5)$$

上列諸式中，等號左邊之各物理變數（即帶有^者）為無因次化後之變數，而等號右邊則為原始變數。然而由於在邊界層內、外之垂直尺度不同（見圖 2），故二種尺度 $\hat{y}$ 及 y' 必須分別提出，以供邊界層修正法使用。本研究提出雙參數之微擾展開，並展開至非線性階（見圖 3），可將均質水流中之速度勢 $\hat{\Phi}^{*(1)}$、軟質底床中三種波之位移勢 $\hat{\Phi}_j^{*(2)}$ (j=1,2,3)、水面波波形 $\hat{\eta}^*$ 及底床床形 $\hat{\xi}^*$ 分別表示如下：

$$\hat{\Phi}^{*(1)} = \varepsilon_1 \hat{\phi}_{10}^* + \varepsilon_1 \varepsilon_2 \hat{\phi}_{11}^* + \varepsilon_1^2 \hat{\phi}_{20}^* + O(\varepsilon_1^2 \varepsilon_2, \ldots), \qquad (6)$$

$$\hat{\Phi}_j^{*(2)} = \varepsilon_1 \hat{\phi}_{10}^{*[j]} + \varepsilon_1 \varepsilon_2 \hat{\phi}_{11}^{*[j]} + \varepsilon_1^2 \hat{\phi}_{20}^{*[j]} + O(\varepsilon_1^2 \varepsilon_2, \ldots), \quad j=1,2,3. \qquad (7)$$

$$\hat{\eta}^* = \varepsilon_1 \hat{\eta}_{10}^* + \varepsilon_1 \varepsilon_2 \hat{\eta}_{11}^* + \varepsilon_1^2 \hat{\eta}_{20}^* + O(\varepsilon_1^2 \varepsilon_2, \ldots), \qquad (8)$$

$$\hat{\xi}^* = \varepsilon_1 \hat{\xi}_{10}^* + \varepsilon_1 \varepsilon_2 \hat{\xi}_{11}^* + \varepsilon_1^2 \hat{\xi}_{20}^* + O(\varepsilon_1^2 \varepsilon_2, \ldots), \qquad (9)$$

上列諸式中顯示對本文所探討之非線性週期波問題僅展開至第三項，此乃避免展開至更高階時將會產生奇異項(secular term)。值得注意的是，由圖 3 可知 ε_2 階並無法單獨存在，此乃因為若無入射波（即無 ε_1），則底床無法產生動力反應，因而 $O(\varepsilon_2^{\,n})$ 各階（$n \geq 1$）的解均為無關緊要解（trivial solution）。就非線性問題而言，上述之泰勒展開式在 $y=0$ 之均質水體與軟質底床交界面處，僅適用於第一種膨脹波及旋轉波，卻不適用於第二種膨脹波，這是因為由於邊界層存在，使得第二種波對垂直尺度之第一階偏導數將產生很大的誤差之故。對孔隙彈性介質底床而言，第二種膨脹波雖然在邊界層外消失了，但其的確存在於邊界層內，因此有必要進一步對第二種膨脹波於邊界層內進行修正，如此才可獲得更完整的解析。考量如圖 2 所示之雙垂直尺度，本研究令 $y' = \hat{y}/\varepsilon_2$ 以放大垂直尺度，修正其第一階偏導數，進而解析第二種膨脹波。

若求解出均質水體之速度勢 $\Phi^{(1)}$ 及孔隙介質底床中之三種位移勢 $\Phi_1^{(2)}$、$\Phi_2^{(2)}$ 及 $\Phi_3^{(2)}$ 之後，其它之物理量如固體結構之有效應力、擾動孔隙水壓力和底床床形即可相繼求得。

三、結果與討論

若考慮一未受孔隙介質底床擾動前具有振幅 a 之入射週期波(即 $\hat{\eta}_{10} = e^{i\hat{x}}$)，其波數為 k_0，選用表 1 之水波、水體和底床孔隙介質，滿足 $\| \varepsilon_1 \|^{y'/2} > \| \varepsilon_2 \| > \| \varepsilon_1 \|^2$ 之條件，經解析後比較軟質有限域底床與半無限域底床之解析解，發現底床床形僅有些微差異，並無太大之不同，表示底床床形受孔隙介質底床厚度改變之影響不明顯（見圖 4）。於擾動孔隙水壓力方面，由於透水孔隙底床厚度之改變，使得孔隙水壓力之分佈與半無限域底床厚度之分佈情形相差甚鉅，如圖 5 所示。圖 5(a)中表孔隙底床厚度（B）為水波波長（L）的四分之一時，顯示不透水剛性邊界之效應，於底部會使得孔隙水壓力變得很大。若透水底床厚度漸漸增大，如圖 5(b)及 5(c)所示，則底部之孔隙水壓力漸漸變小，且愈接近於半無限域之分佈情形，當透水孔隙底床厚度與水波波長相等時(見圖 5(d))，則孔隙水壓力之分佈已和半無限域底床之孔隙水壓力分佈完全相同。而孔隙介質之垂直方向上的有效應力 τ_{yy}（見圖 6），亦受不透水剛性邊界之影響，於底部變得很大（見圖 6(a)）。若透水底床厚度漸漸增大，如圖 6(b)及 6(c)所示，則底部之垂直有效應力漸漸變小，且愈接近於半無限域之應力分佈情形，當透水孔隙底床厚度與水波波長相等時（見圖 6(d)），則垂直方向上的有效應力分佈已與半無限域底床之垂直方向上的有效應力分佈十分接近。

四、結論

本研究提出二微小尺度($\varepsilon_1, \varepsilon_2$)，進行雙參數之微擾展開，並以邊界層修正法修正第二種膨脹波，使得解決有限域軟孔隙

彈性介質底床變形之方法更完整、更有系統。本研究將軟孔隙介質有限域底床與半無限域底床之解析解進行比較，結果發現底床床形僅有些微差異，表示底床床形不太受孔隙介質底床厚度改變之影響。而擾動孔隙水壓力及孔隙介質之垂直有效應力，受不透水剛性邊界之影響顯著，當透水底床厚度不大時，孔隙水壓和垂直有效應力於底部會變得很大。當透水底床厚度漸漸增大，則其結果愈接近於半無限域之分佈情形，充分顯示本解之正確性。

謝誌

本研究承蒙 行政院國家科學委員會補助經費，特此致謝！

參考文獻

Biot, M. A., 1956. Theory of propagation elastic waves in a fluid saturated porous solid I: Low-frequency range. JASA 28, pp.168-178.

Chen, T.W., Huang, L.H., and Song, C.H., 1997. Dynamic response of poroelastic bed to nonlinear water waves. J. Engrg. Mech., ASCE, 123(10): pp. 1041-1049.

Dagan, G., 1979. The generalization of Darcy's law for nonuniform flows. Water Resour. Res., 15, pp. 1-17.

Dean, R.G. and Dalrymple, R.A., 1991. *Water wave mechanics for engineers and scientists*. World Scientific, Singapore.

Fenton, J.D., 1985. A fifth order Stokes theory for steady waves. J. Waterway, Port, Coastal and Ocean Engr., ASCE, Vol. 111, No. 2, pp. 216-233.

Huang, L.H. and Chwang, A.T., 1990. Trapping and absorption of sound waves. II: A sphere covered with a porous layer. Wave Motion, 12: pp. 401-414.

Huang, L.H. and Song, C.H., 1993. Dynamic response of poroelastic bed to water waves. J. Hydraul. Engrg., ASCE, 119: pp. 1003-1020.

Liu, P.L.-F. and Dalrymple, R.A., 1984. The damping of water waves due to percolation. Coast. Engrg. Vol. 8, pp. 33-49.

Mei, C.C., 1983. *The Applied Dynamics of Ocean Waves*. John Wiely & Sons, New York.

Verruijt, A., 1969. Elastic storage of aquifers. *Flow through porous media*. De DeWiest, R. J. M. (Ed.), Academic Press.

黃良雄，1998。海域地形變遷—泥沙底床流動動力反應之邊界層分析（二）。國科會報告 NSC87-2611-E002-001。

謝平城，1999。軟孔隙彈性介質底床之流體動力反應。國立台灣大學土木工程學研究所博士論文。

表 1 軟孔隙介質及水波之選用條件

Items	Values	Units
Water		
density	1000	kg/m^3
bulk modulus	2.3×10^9	N/m^2
viscosity	0.001	Ns/m^2
depth	0.5	m
wave amplitude	0.092	m
period	1.55	s
Skeleton		
density	2650	kg/m^3
Lame's constant	5.0×10^4	N/m^2
Lame's constant	1.0×10^5	N/m^2
specific permeability	1.0×10^{-11}	m^2
porosity	0.4	

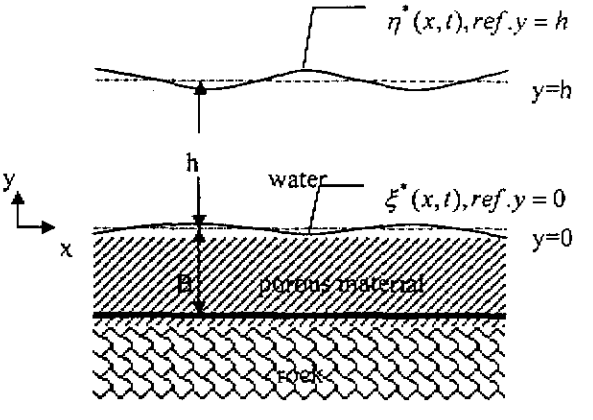

圖 1 有限域孔隙介質底床受水波作用之示意

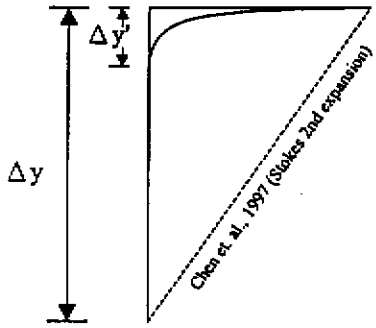

圖 2 邊界層內第二種膨脹波之雙尺度示意

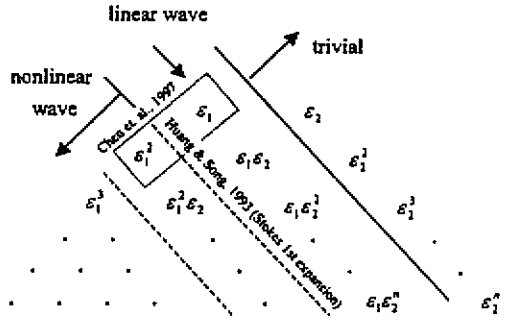

圖 3 雙參數微擾法展開之示意

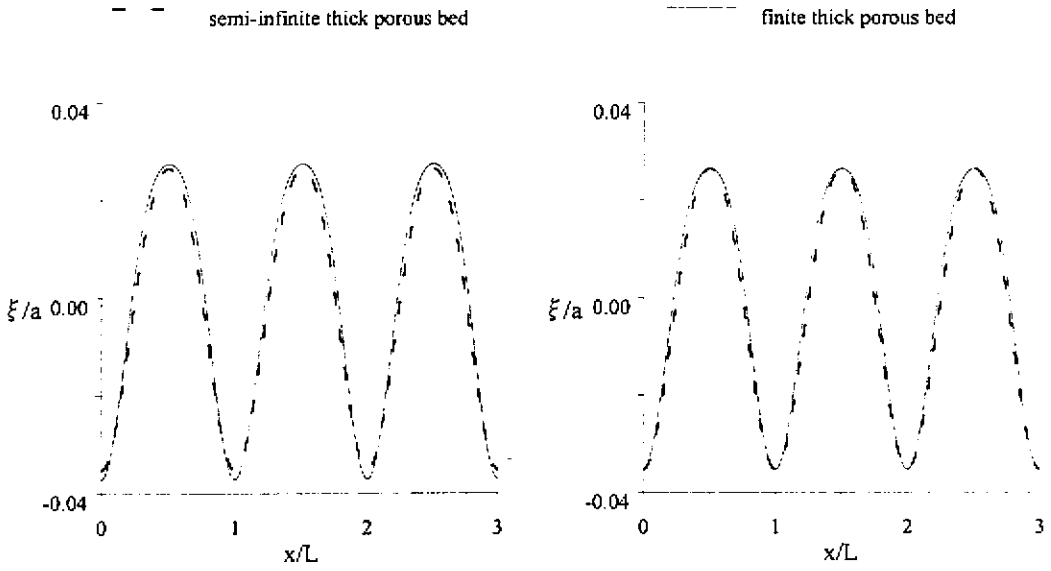

圖 4 重力水波衍生之底床床形變化

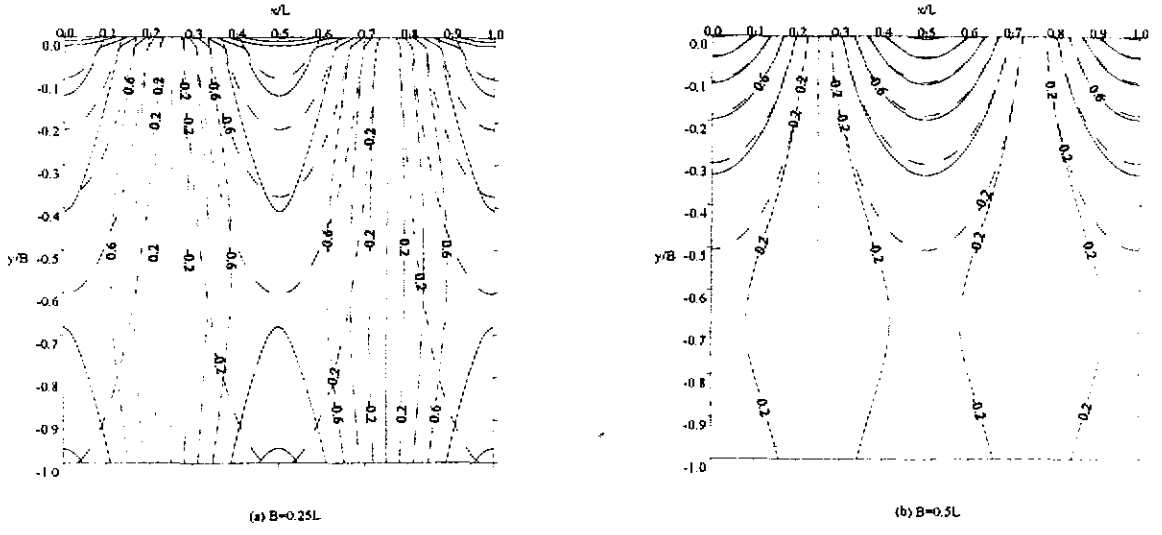

finite thick porous bed

semi-infinite thick porous bed

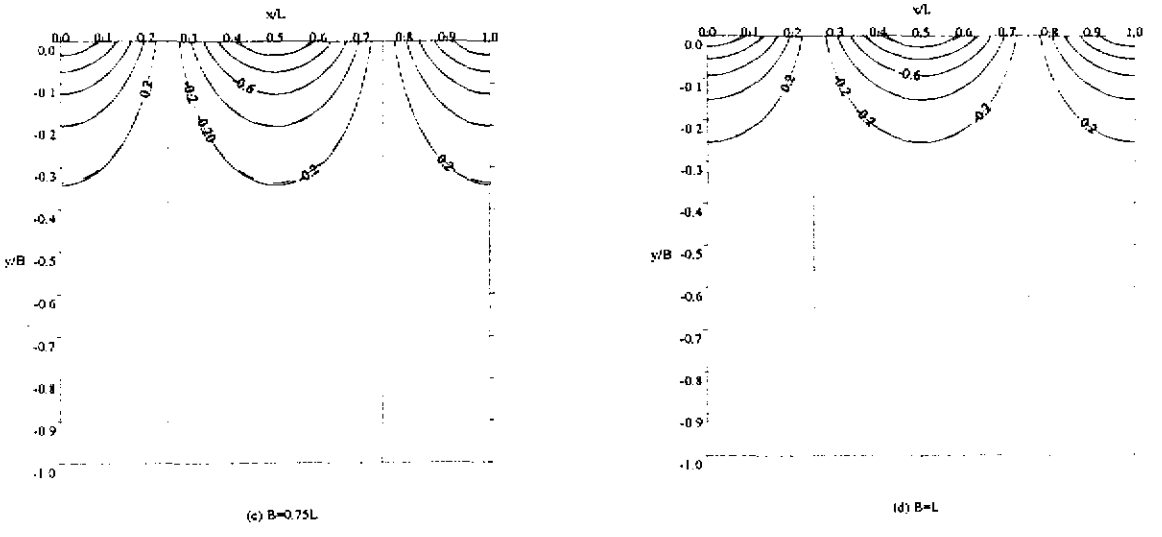

圖 5 重力水波衍生之底床擾動水壓力之分佈

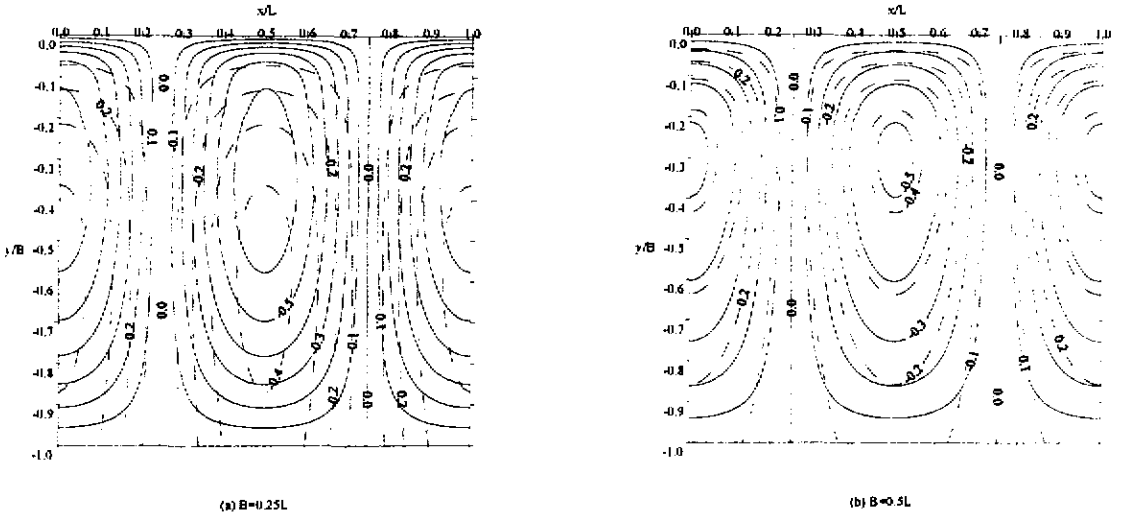

finite thick porous bed

semi-infinite thick porous bed

圖 6 重力水波衍生之底床垂直有效應力之分佈

EFFECTS OF NONLINEAR WATER WAVES ON A SOFT POROELASTIC BED WITH FINITE THICKNESS

By Ping-cheng Hsieh[1] and Liang-hsiung Huang[2], Associate Member, ASCE

Key Words : boundary layer correction; two-parameter perturbation expansion; boundary effect; soft finite thickness poloelastic bed

ABSTRACT: Since the porous material is usually finite thickness in the nature, the effects of periodically nonlinear water waves propagating over a soft poroelastic bed with finite thickness are hence noticed and studied in this work. The water waves are simulated by potential theory while the porous bed is governed by Biot's theory of poroelasticity (1956) herein. The conventional Stokes expansion of water waves based on a one-parameter perturbation expansion fails to solve the soft poroelastic bed problem; therefore, the boundary layer correction approach combined with a two-parameter perturbation expansion is proposed, and which enables us to solve the problem of soft poroelastic bed with finite thickness. The results are compared to the similar problem with infinite thickness porous bed. The boundary effects of the impervious rock are significant on wave-induced pore water pressure and effective stresses, but very little on wave profiles at the free surface and the porous bed surface. However, the rigid boundary is insignificant to the pore water pressure and effective stresses when the thickness of porous bed is larger than about one wavelength.

INTRODUCTION

The dynamic response of propagating water wave acting on coastal constructions is quite emphasized during the design work especially in the analysis of seabed instability. The wave-induced variation in pore pressure and effective stresses has been recognized as a major factor for destroying the stability of the seabed so that it is very important to correctly estimate

[1]Assistant Professor, Department of Soil and Water Conservation, National Chung-Hsing University, Taichung, 40227, Taiwan, ROC. To whom all correspondence should be addressed. E-mail: pchsieh@dragon.nchu.edu.tw
[2]Professor, Department of Civil Engineering, National Taiwan University, Taipei, 106, Taiwan, ROC.

the pore pressure and effective stresses inside the seabed.

At the early stage, most researchers only study the linear or nonlinear water waves acting on a seabed that was usually assumed to be rigid material, no matter it was considered as permeable (Putnam, 1949; Reid and Kajiura, 1957; Sleath, 1970; Moshagen and Torum, 1975) or impermeable (Mei, 1983; Fenton, 1985; Dean and Dalrymple, 1991). Actually, fluid within the porous material interacting with deforming solid skeleton is very obvious, and thus a realistic analysis based on deformable porous seabed is necessary.

Biot (1956) developed a theory of poroelasticity to discuss elastic wave in a fluid-saturated porous solid. Huang and Chwang (1990) investigated Biot's oscillatory equation for acoustic problem without simplifications and obtained three decoupled Helmoltz equations standing for three kinds of wave—two longitudinal waves and one transverse wave. Following this method, Huang and Song (1993) then analytically solved the problem of periodically linear water waves interacting with a deformable bed by treating the bed as a poroelastic material. Their approach was quite successful in revealing most physical mechanisms by using potential water wave and Darcy's porous medium flow. Chen et al. (1997) further applied the conventional Stokes expansion of nonlinear deepwater wave based on $\varepsilon_1 = k_0 a$ to investigate the dynamic response of a deformable permeable seabed. They found that Stokes expansion is only valid for the hard poroelastic material but invalid for the soft one even though the Ursell parameter is small. Finally, Hsieh et al. (2000) proposed a two-parameter perturbation method and a boundary layer correction approach to carry out the analytic solution of nonlinear water waves propagating over a soft poroelastic material bed with infinite thickness. Note that Huang and Song (1993), Chen et al. (1997), and Hsieh et al. (2000) all focused on poroelastic bed with infinite thickness.

Based on the fact that the seabed is generally multi-layered and the nonlinear water waves are very likely to happen, the present study will find a way to investigate the complicated finite

depth problem and the interaction between the nonlinear water waves and the poroelastic material seabed with a single layer, i.e. the thickness of the porous bed is finite. The present work is aimed at investigating the boundary effect of a soft poroelastic seabed under periodically nonlinear water waves propagation.

MATHEMATICAL FORMULATION

The plane water waves, as indicated in Fig. 1, propagating over a horizontally finite thickness homogeneous poroelastic bed, are simulated by potential theory and the porous medium saturated with water is governed by Biot's theory of poroelasticity (1956). The region (1) ranges from $y=\xi^*(x,t)$ to $y=h+\eta^*(x,t)$, and the region (2) from $y=\xi^*(x,t)$ to $y=-B$. The symbols η^* and ξ^* are the displacements of waves from the mean free surface ($y=h$) and the mean surface of porous bed ($y=0$), respectively.

Boundary-Value Problem

Assuming that the homogeneous flow, region (1) of Fig. 1, is potential flow, the velocity $u^{*(1)}$ can be represented by velocity potential $\Phi^{*(1)}$ as

$$u^{*(1)}=\nabla\Phi^{*(1)}. \tag{1}$$

The equations of continuity and momentum in terms of velocity potential hence become

$$\nabla^2\Phi^{*(1)}=0, \tag{2}$$

$$\rho_0\frac{\partial\Phi^{*(1)}}{\partial t}+\frac{\rho_0}{2}\left\{\left[\frac{\partial\Phi^{*(1)}}{\partial x}\right]^2+\left[\frac{\partial\Phi^{*(1)}}{\partial y}\right]^2\right\}+P^{*(1)}=0, \tag{3}$$

where $P^{*(1)}$ is the wave-induced pressure in region (1), and ρ_0 is the density of water.

Referring to Huang and Chwang (1990), the linear momentum equations of solid skeleton and fluid for the porous bed based on the theory of poroelasticity may be written as

$$\nabla\cdot\underline{\underline{\sigma}}^*=\rho_{11}\frac{\partial^2 d^*}{\partial t^2}+\rho_{12}\frac{\partial^2 D^*}{\partial t^2}+b\left(\frac{\partial d^*}{\partial t}-\frac{\partial D^*}{\partial t}\right), \tag{4}$$

$$\nabla \cdot \underline{\underline{S}}^{*} = \rho_{12} \frac{\partial^2 \underline{d}^{*}}{\partial t^2} + \rho_{22} \frac{\partial^2 \underline{D}^{*}}{\partial t^2} - b\left(\frac{\partial \underline{d}^{*}}{\partial t} - \frac{\partial \underline{D}^{*}}{\partial t} \right), \tag{5}$$

with

$$\underline{\underline{\sigma}}^{*} = \underline{\underline{\tau}}^{*} - (1 - n_0)\mathrm{P}^{*(2)}\underline{\underline{\mathrm{I}}}, \tag{6}$$

$$\underline{\underline{\tau}}^{*} = 2G\underline{\underline{e}}^{*} + \lambda(\nabla \cdot \underline{d}^{*})\underline{\underline{\mathrm{I}}}, \tag{7}$$

$$\underline{\underline{e}}^{*} = \frac{1}{2}\left[\nabla \underline{d}^{*} + (\nabla \underline{d}^{*})^{t}\right], \tag{8}$$

$$\underline{\underline{S}}^{*} = -n_0 \mathrm{P}^{*(2)}\underline{\underline{\mathrm{I}}}, \tag{9}$$

$$\rho_{11} = (1 - n_0)\rho_s + \rho_a, \tag{10}$$

$$\rho_{12} = -\rho_a, \tag{11}$$

$$\rho_{22} = n_0 \rho_0 + \rho_a, \tag{12}$$

$$b = \mu n_0^{\,2} / k_p, \tag{13}$$

where $\underline{\underline{\sigma}}^{*}$ is the total stress tensor of solid; $\underline{\underline{\tau}}^{*}$ is the effective stress tensor of solid; $\underline{\underline{S}}^{*}$ is the normal stress tensor of fluid; $\underline{d}^{*}$ and $\underline{D}^{*}$ are the displacements of solid and fluid, respectively; $\mathrm{P}^{*(2)}$ is the wave-induced pore water pressure; ρ_s is the density of solid; ρ_a is the mass coupling effect (neglected in this study); n_0 is the porosity; μ is the viscosity of fluid; k_p is the specific permeability; G and λ are Lame constants of elasticity; $\underline{\underline{\mathrm{I}}}$ is the identity matrix.

Combining continuity equations of solid and fluid with state equation of fluid and after linearization of the porosity (Verruijt, 1969), we can find

$$\frac{\partial \mathrm{P}^{*(2)}}{\partial t} = -\frac{K}{n_0}\left[(1 - n_0)\nabla \cdot \left(\frac{\partial \underline{d}^{*}}{\partial t}\right) + n_0 \nabla \cdot \left(\frac{\partial \underline{D}^{*}}{\partial t}\right)\right], \tag{14}$$

for waved-induced pore water pressure. In (14), K is the bulk modulus of compressibility of

fluid inside the porous bed.

There are three boundaries (i)free surface $\left[y = h + \eta^*(x,t)\right]$, (ii)porous bed interface $\left[y = \xi^*(x,t)\right]$, and (iii)poroelastic bed/impervious rock interface $\left[y = -B\right]$ in this study, which, referring to Deresiewicz and Skalak (1963), are required to satisfy the following boundary conditions.

At the free surface, a kinematic boundary condition exists as

$$-\frac{\partial \eta^*}{\partial x}\frac{\partial \Phi^{*(1)}}{\partial x} + \frac{\partial \Phi^{*(1)}}{\partial y} = \frac{\partial \eta^*}{\partial t}, \tag{15}$$

and a dynamic boundary condition exists as

$$\frac{\partial \Phi^{*(1)}}{\partial t} + \frac{1}{2}\left\{\left[\frac{\partial \Phi^{*(1)}}{\partial x}\right]^2 + \left[\frac{\partial \Phi^{*(1)}}{\partial y}\right]^2\right\} + g\eta^* = 0. \tag{16}$$

At the porous bed surface, the continuity of pressure for fluid gives

$$P^{*(1)} = P^{*(2)}, \tag{17}$$

and the continuity of fluid flux gives

$$\underline{n}_2^* \cdot \left[(1-n_0)\frac{\partial \underline{d}^*}{\partial t} + n_0 \frac{\partial \underline{D}^*}{\partial t}\right] = \underline{n}_2^* \cdot \nabla \Phi^{*(1)}, \tag{18}$$

where

$$\underline{n}_2^* = \left(\frac{-\partial \xi^*}{\partial x}, 1\right) \Big/ \sqrt{1 + \left(\frac{\partial \xi^*}{\partial x}\right)^2} \tag{19}$$

is the unit normal vector at the porous bed surface. Considering the kinematics of this surface, we have

$$\frac{\partial \xi^*}{\partial t} = \frac{\partial \underline{d}^*}{\partial t} \cdot \left(-\frac{\partial \xi^*}{\partial x}, 1\right), \tag{20}$$

and (20) will be used to solve ξ^*. And the continuity of effective stresses of solid gives

$$\underline{n}_2^* \cdot \underline{\underline{\tau}}^* = 0. \tag{21}$$

At the interface between the porous bed and the impervious rock, $y=-B$, the boundary conditions are no displacement for porous material

$$d^* = 0, \tag{22}$$

and no flux for fluid

$$u_{2y}^* = 0, \tag{23}$$

where u_{2y}^* is the vertical component of the velocity of fluid within the porous bed.

If both $|\eta^*|$ and $|\xi^*|$ are much smaller than the relative wavelengths, it is more convenient to shift the boundary conditions at the free surface, $y=h+\eta^*(x,t)$, and at the porous bed surface, $y=\xi^*(x,t)$, to $y=h$ and $y=0$ first before solving the boundary value problem. Conventionally, Taylor series expansions are applied to the boundary conditions at the free surface [(15) and (16)] and at the porous bed surface [(17), (18), (21) and (20)] by performing

$$\sum_{m=0}^{\infty} \frac{(\eta^*)^m}{m!} \frac{\partial^m}{\partial y^m} \quad \text{and} \quad \sum_{m=0}^{\infty} \frac{(\xi^*)^m}{m!} \frac{\partial^m}{\partial y^m},$$

respectively before liquefaction.

As will be indicated by (36), for the present problem, due to the existence of the second longitudinal wave inside the boundary layer of the soft poroelastic bed, the above Taylor series expansions at the interface ($y=0$) are applicable for the first longitudinal wave and the transverse wave, but not applicable for the second longitudinal wave because the effect of the boundary layer will render errors of the partial derivative in the vertical direction for the second longitudinal wave. That's why Chen et al. (1997) failed to solve the nonlinear problem for soft porous material by only one length scale. To overcome the difficulty, another small parameter $\varepsilon_2 = k_0/k_2$ other than $\varepsilon_1 = k_0 a$ needs to be proposed. Thus, the vertical coordinate y for the second longitudinal wave will be enlarged into y' based on this small parameter ε_2 (see (40b)).

Referring to Huang and Song (1993) for the decoupling processes of Biot's equations of poroelasticity (1956), the governing equations (4) and (5) can be rewritten into three decoupled scalar equations as

$$\nabla^2\Phi_j^{*(2)} + k_j^2\Phi_j^{*(2)} = 0, \qquad \text{j=1,2,3.} \tag{24}$$

Also, (14) of the wave-induced pore water pressure gives

$$P^{*(2)} = \frac{K}{n_0}\left[(1-n_0+\alpha_1 n_0)k_1^2\Phi_1^{*(2)} + (1-n_0+\alpha_2 n_0)k_2^2\Phi_2^{*(2)}\right], \tag{25}$$

where wave numbers k_j and solid/fluid related parameters α_j are given as (8)-(20) in Huang and Song (1993). In (24), $\Phi_1^{(2)}$ and $\Phi_2^{(2)}$ are the displacement potentials of the first and the second longitudinal waves, respectively; while $\Phi_3^{(2)}$ is the displacement potential of the transverse wave, i.e.

$$d^* = \nabla\Phi_1^{*(2)} + \nabla\Phi_2^{*(2)} + \nabla\wedge(\Phi_3^{*(2)}e_z), \tag{26}$$

$$D^* = \alpha_1\nabla\Phi_1^{*(2)} + \alpha_2\nabla\Phi_2^{*(2)} + \alpha_3\nabla\wedge(\Phi_3^{*(2)}e_z). \tag{27}$$

Note that governing equations (2) and (24), wave-induced pressure and effective stresses (3), (25), and (7), together with boundary conditions (15), (16), (17), (18), (21), (22) and (23) form the complete boundary value problem of the present study. ((20) is used to find ξ^* only, and the vertical component of (22) is identical to (23) in the present study.)

Nondimensionalization of Variables

Huang and Song (1993) defined the following parameters

$$m = (2G+\lambda)n_0/K, \tag{28}$$

$$\varepsilon = n_0\rho_0\omega/b, \tag{29}$$

$$\Lambda^2 = \frac{n_0\rho_0 + (1-n_0)\rho_s}{2G+\lambda+(K/n_0)}\frac{\omega^2}{k_0^2}, \tag{30}$$

$$\Pi^2 = \frac{i(m+1)}{m\varepsilon}\frac{\rho_0}{K}\frac{\omega^2}{k_0^2}, \tag{31}$$

$$\Psi^2 = \frac{n_0\rho_0 + (1-n_0)\rho_s}{G}\frac{\omega^2}{k_0^2}, \tag{32}$$

in their solution of linear water waves propagating over a poroelastic bed. In which, ε is called penetrability parameter; ω is the frequency; m is the stiffness ratio of solid and fluid; k_0 is the wave number of water wave and will be found as complex; Λ and Ψ are only functions of water wave speed and material (fluid and solid skeleton) properties, while Π is not only a function of the same variables for Λ and Ψ but also depends on the permeability of porous medium.

For low penetrability, i.e. $\|\varepsilon\| << 1$, (30)-(32) could be simplified to

$$\Lambda^2 \doteqdot (k_1/k_0)^2, \tag{33}$$

$$\Pi^2 \doteqdot (k_2/k_0)^2, \tag{34}$$

$$\Psi^2 \doteqdot (k_3/k_0)^2. \tag{35}$$

Moreover, for soft solid skeleton, $\|k_2\| >> \|k_0\|$ is discovered and that $\|\Pi^2\| \doteqdot \|k_2^2/k_0^2\| >> 1$ is used to define the "soft" material in this study. Since $\|\Lambda^2\|$ is always smaller than $\|\Psi^2\|$ (see (30) and (32)), we can obtain

$$\|\Lambda^2\| < \|\Psi^2\| << 1 << \|\Pi^2\|. \tag{36}$$

Based on the above discussion, we herewith define

$$\varepsilon_1 = k_0 a, \tag{37}$$

$$\varepsilon_2 = k_0/k_2 \tag{38}$$

for later use. Where a is the amplitude of incoming water wave.

After the analysis of order of magnitude for each dependent variable, the dimensionless

variables are selected as

$$\hat{x} = k_0 x\,, \tag{39}$$

$$\hat{y} = k_0 y\,, \tag{40a}$$

$y' = \hat{y}/\varepsilon_2$, for the second longitudinal wave only, (40b)

$$\hat{t} = \sqrt{gk_0}\,t\,, \tag{41}$$

$$\hat{\eta}^* = k_0 \eta^*\,, \tag{42}$$

$$\hat{\omega} = \omega/\sqrt{gk_0}\,, \tag{43}$$

$$\hat{\Phi}^{*(1)} = \frac{k_0^{\,2}}{\sqrt{gk_0}}\Phi^{*(1)}, \tag{44}$$

$$\hat{\Phi}_1^{*(2)} = e^{k_0 h} k_0^{\,2} \Phi_1^{*(2)}\,, \tag{45}$$

$$\hat{\Phi}_2^{*(2)} = e^{k_0 h} k_0^{\,2} \frac{k_2^2}{k_1^2}\Phi_2^{*(2)} = \frac{e^{k_0 h} k_0^2}{\varepsilon_2^2 \Lambda^2}\Phi_2^{*(2)}, \tag{46}$$

$$\hat{\Phi}_3^{*(2)} = e^{k_0 h} k_0^{\,2} \Phi_3^{*(2)}, \tag{47}$$

$$\hat{\xi}^* = \frac{k_0 e^{k_0 h}}{\Psi^2}\xi^*, \tag{48}$$

$$\hat{\mathrm{P}}^{*(1)} = \frac{k_0}{\rho_0 g}\mathrm{P}^{*(1)}, \tag{49}$$

$$\hat{\mathrm{P}}^{*(2)} = \frac{k_0}{\rho_0 g}\mathrm{P}^{*(2)}. \tag{50}$$

All the symbols of variables on the left-hand side of (39)-(50) are dimensionless, but those on the right-hand side are dimensional. Note that since vertical length scales need multiple scales (see Fig. 2), $\hat{y}$ and y' are proposed.

Applying the two-parameter perturbation expansion (see Fig. 3), velocity potential of flow and displacement potentials of the first longitudinal wave and the transverse wave for the whole domain can be written as

$$\hat{\Phi}^{*(1)} = \varepsilon_1 \hat{\phi}^*_{10} + \varepsilon_1 \varepsilon_2 \hat{\phi}^*_{11} + \varepsilon_1^2 \hat{\phi}^*_{20} + O(\varepsilon_1^2 \varepsilon_2, ...), \tag{51}$$

$$\hat{\Phi}^{*(2)}_j = \varepsilon_1 \hat{\phi}^{*[j]}_{10} + \varepsilon_1 \varepsilon_2 \hat{\phi}^{*[j]}_{11} + \varepsilon_1^2 \hat{\phi}^{*[j]}_{20} + O(\varepsilon_1^2 \varepsilon_2, ...), \quad j=1,3. \tag{52}$$

Due to (36), the second longitudinal wave needs to be solved inside the boundary layer, and thus its displacement potential is nondimensionalized especially as (46) and expanded as

$$\hat{\Phi}^{*(2)}_2 = \varepsilon_1 \hat{\phi}^{*[2]}_{10} + \varepsilon_1 \varepsilon_2 \hat{\phi}^{*[2]}_{11} + \varepsilon_1^2 \hat{\phi}^{*[2]}_{20} + O(\varepsilon_1^2 \varepsilon_2, ...), \tag{53}$$

if $\|\varepsilon_2\|$ and $\|\varepsilon_1\|$ are smaller than unity. Also, the water wave profile at the free surface becomes

$$\hat{\eta}^* = \varepsilon_1 \hat{\eta}^*_{10} + \varepsilon_1 \varepsilon_2 \hat{\eta}^*_{11} + \varepsilon_1^2 \hat{\eta}^*_{20} + O(\varepsilon_1^2 \varepsilon_2, ...), \tag{54}$$

and the wave profile of the porous bed surface becomes

$$\hat{\xi}^* = \varepsilon_1 \hat{\xi}^*_{10} + \varepsilon_1 \varepsilon_2 \hat{\xi}^*_{11} + \varepsilon_1^2 \hat{\xi}^*_{20} + O(\varepsilon_1^2 \varepsilon_2, ...). \tag{55}$$

For a periodic motion with frequency ω, the aforementioned variables $[\,]^*(R,t)$ can be written as $[\,](R)e^{-i\omega t}$, where R is the position vector. Let the given incoming-wave amplitude before being disturbed by the porous bed be a (i.e. $\hat{\eta}_{10} = e^{iR}$), Stokes expansion based on ε_1 and ε_2 will be carried out only to the first three terms for the present nonlinear water wave problem to avoid the occurrence of secular terms. Thus, after Taylor series expansions at the free surface and at the porous bed surface respectively are applied, the boundary value problem of each order without the time factor is obtained in the following.

Boundary Value Problem Without the Boundary Layer

Since the first longitudinal wave and the transverse wave propagate throughout the whole domain, i.e. both inside and outside the boundary layer, there is no necessity to make any correction of these two waves. Hence the boundary value problem without the boundary layer is formulated as follows:

$O(\varepsilon_1)$

Governing equations

region (1): $-\infty < \hat{x} < \infty,\quad 0 < \hat{y} < k_o h,$

$$\hat{\nabla}^2 \hat{\phi}_{10} = 0; \tag{56}$$

region (2): $-\infty < \hat{x} < \infty,\quad -\infty < \hat{y} < 0,$

$$\hat{\nabla}^2 \hat{\phi}_{10}^{[1]} + \Lambda^2 \hat{\phi}_{10}^{[1]} = 0, \tag{57}$$

$$\hat{\nabla}^2 \hat{\phi}_{10}^{[3]} + \Psi^2 \hat{\phi}_{10}^{[3]} = 0. \tag{58}$$

Boundary conditions

at the free surface: $\hat{y} = k_0 h,\ -\infty < \hat{x} < \infty,$

(a) kinematic free surface boundary condition

$$\hat{\phi}_{10,\hat{y}} = -i\hat{\omega}\hat{\eta}_{10}, \tag{59}$$

(b) dynamic free surface boundary condition

$$i\hat{\omega}\hat{\phi}_{10} = \hat{\eta}_{10}; \tag{60}$$

at the porous bed surface: $\hat{y} = 0,\ -\infty < \hat{x} < \infty,$

(a) continuity of pressure

$$i\hat{\omega}\hat{\phi}_{10} - \frac{k_0 K \Lambda^2}{e^{k_0 h} n_0 \rho_0 g} q_1 \hat{\phi}_{10}^{[1]} = 0, \tag{61}$$

(b) continuity of flux

$$i\hat{\omega} q_1 \hat{\phi}_{10,\hat{y}}^{[1]} - i\hat{\omega} q_3 \hat{\phi}_{10,\hat{x}}^{[3]} + e^{k_0 h} \hat{\phi}_{10,\hat{y}} = 0, \tag{62}$$

(c) continuity of effective stress (only $\tau_{\hat{x}\hat{y}} \fallingdotseq 0$)

$$2\hat{\phi}_{10,\hat{x}\hat{y}}^{[1]} + \hat{\phi}_{10,\hat{y}\hat{y}}^{[3]} - \hat{\phi}_{10,\hat{x}\hat{x}}^{[3]} = 0; \tag{63}$$

at the porous material/impervious rock interface: $\hat{y} = -k_0 B,\ -\infty < \hat{x} < \infty,$

(a) no horizontal displacement for porous material

$$\hat{\phi}_{10,x}^{[1]} + \hat{\phi}_{10,y}^{[3]} = 0, \tag{64}$$

(b) no flux for fluid

$$\alpha_1\hat{\phi}^{[1]}_{10,\hat{y}} - \alpha_3\hat{\phi}^{[3]}_{10,\hat{x}} = 0. \tag{65}$$

where

$$q_j = 1 - n_0 + \alpha_j n_0, \quad \text{j=1,3.} \tag{66}$$

Note that only one component of the above boundary condition of continuity of effective stresses is needed, i.e. $\tau_{\hat{x}\hat{y}} \doteq 0$, otherwise it will become overdetermined. (Another condition, $\tau_{\hat{y}\hat{y}} \doteq 0$, includes the effect of the second longitudinal wave and which will be adopted by the boundary layer correction for the second longitudinal wave later.) And, since for the low penetrability of the porous material, both α_1 and α_3 are very close to unity, the boundary condition of no flux for fluid is equivalent to that of no vertical displacement of the soft porous material, therefore only one is needed. Herein, the former is selected.

$O(\varepsilon_1\varepsilon_2)$

Governing equations

region (1): $-\infty < \hat{x} < \infty, \quad 0 < \hat{y} < k_0 h,$

$$\hat{\nabla}^2\hat{\phi}_{11} = 0; \tag{67}$$

region (2): $-\infty < \hat{x} < \infty, \quad -\infty < \hat{y} < 0,$

$$\hat{\nabla}^2\hat{\phi}^{[1]}_{11} + \Lambda^2\hat{\phi}^{[1]}_{11} = 0, \tag{68}$$

$$\hat{\nabla}^2\hat{\phi}^{[3]}_{11} + \Psi^2\hat{\phi}^{[3]}_{11} = 0. \tag{69}$$

Boundary conditions

at the free surface: $\hat{y} = k_0 h, \quad -\infty < \hat{x} < \infty,$

(a) kinematic free surface boundary condition

$$\hat{\phi}_{11,\hat{y}} = -i\hat{\omega}\hat{\eta}_{11}, \tag{70}$$

(b) dynamic free surface boundary condition

$$i\hat{\omega}\hat{\phi}_{11} = \hat{\eta}_{11}\,; \tag{71}$$

at the porous bed surface: $\hat{y} = 0\,,\ -\infty < \hat{x} < \infty,$

(a) continuity of pressure

$$i\hat{\omega}\hat{\phi}_{11} - \frac{k_0 K\Lambda^2}{e^{k_0 h} n_0 \rho_0 g} q_1 \hat{\phi}_{11}^{[1]} = 0\,, \tag{72}$$

(b) continuity of flux

$$i\hat{\omega}e^{-k_0 h}\left(q_1\hat{\phi}_{11,\hat{y}}^{[1]} - q_3\hat{\phi}_{11,\hat{x}}^{[3]}\right) + \hat{\phi}_{11,\hat{y}} = 0\,, \tag{73}$$

(c) continuity of effective stress (only $\tau_{\hat{x}\hat{y}} \fallingdotseq 0$)

$$2\hat{\phi}_{11,\hat{x}\hat{y}}^{[1]} + \hat{\phi}_{11,\hat{y}\hat{y}}^{[3]} - \hat{\phi}_{11,\hat{x}\hat{x}}^{[3]} = 0\,; \tag{74}$$

at the porous material/impervious rock interface: $\hat{y} = -k_0 B\,,\ -\infty < \hat{x} < \infty,$

(a) no horizontal displacement for porous material

$$\hat{\phi}_{11,\hat{x}}^{[1]} + \hat{\phi}_{11,\hat{y}}^{[3]} = 0, \tag{75}$$

(a) no flux for fluid

$$\alpha_1\hat{\phi}_{11,\hat{y}}^{[1]} - \alpha_3\hat{\phi}_{11,\hat{x}}^{[3]} = 0. \tag{76}$$

Again, only one component of the boundary condition of continuity of effective stresses is needed, i.e. $\tau_{\hat{x}\hat{y}} \fallingdotseq 0$, for the same reason mentioned above, and vanishing vertical solid displacement is equivalent to vanishing fluid flux at impervious boundary.

$O\left(\varepsilon_1^2\right)$

Governing equations

region (1): $-\infty < \hat{x} < \infty,\ \ 0 < \hat{y} < k_0 h\,,$

$$\hat{\nabla}^2\hat{\phi}_{20} = 0\,; \tag{77}$$

region (2): $-\infty < \hat{x} < \infty,\ \ -\infty < \hat{y} < 0\,,$

$$\hat{\nabla}^2\hat{\phi}_{20}^{[1]}+\frac{\widetilde{k}_1^2}{k_1^2}\Lambda^2\hat{\phi}_{20}^{[1]}=0, \tag{78}$$

$$\hat{\nabla}^2\hat{\phi}_{20}^{[3]}+\frac{\widetilde{k}_3^2}{k_3^2}\Psi^2\hat{\phi}_{20}^{[3]}=0. \tag{79}$$

Boundary conditions

at the free surface: $\hat{y}=k_0h$, $-\infty<\hat{x}<\infty$,

(a) kinematic free surface boundary condition

$$\hat{\phi}_{20,\hat{y}}+2i\hat{\omega}\hat{\eta}_{20}=\hat{\eta}_{10,\hat{x}}\hat{\phi}_{10,\hat{x}}-\hat{\eta}_{10}\hat{\phi}_{10,\hat{y}\hat{y}}, \tag{80}$$

(b) dynamic free surface boundary condition

$$2i\hat{\omega}\hat{\phi}_{20}-\hat{\eta}_{20}=\frac{1}{2}\left(\hat{\phi}_{10,\hat{x}}^2+\hat{\phi}_{10,\hat{y}}^2\right)-i\hat{\omega}\hat{\eta}_{10}\hat{\phi}_{10,\hat{y}}; \tag{81}$$

at the porous bed surface: $\hat{y}=0$, $-\infty<\hat{x}<\infty$,

(a) continuity of pressure

$$2i\hat{\omega}\hat{\phi}_{20}-\frac{k_0K\Lambda^2}{e^{k_0h}n_0\rho_0g}\widetilde{q}_1\hat{\phi}_{20}^{[1]}=\frac{1}{2}\left(\hat{\phi}_{10,\hat{x}}^2+\hat{\phi}_{10,\hat{y}}^2\right)-\frac{i\hat{\omega}\Psi^2\hat{\xi}_{10}}{e^{k_0h}}\hat{\phi}_{10,\hat{y}}+\frac{\Psi^2k_0K\Lambda^2\hat{\xi}_{10}}{e^{2k_0h}n_0\rho_0g}q_1\hat{\phi}_{10,\hat{y}}^{[1]}, \tag{82}$$

(b) continuity of flux

$$e^{k_0h}\hat{\phi}_{20,\hat{y}}+2i\hat{\omega}\left(\widetilde{q}_1\hat{\phi}_{20,\hat{y}}^{[1]}-\widetilde{q}_3\phi_{20,\hat{x}}^{[3]}\right)=\Psi^2\hat{\xi}_{10,\hat{x}}\hat{\phi}_{10,\hat{x}}-\Psi^2\hat{\xi}_{10}\hat{\phi}_{10,\hat{y}\hat{y}}$$

$$+i\hat{\omega}\Psi^2e^{-k_0h}\hat{\xi}_{10,\hat{x}}\left(q_1\hat{\phi}_{10,\hat{x}}^{[1]}+q_3\hat{\phi}_{10,\hat{y}}^{[3]}\right)-i\hat{\omega}\Psi^2e^{-k_0h}\hat{\xi}_{10}\left(q_1\hat{\phi}_{10,\hat{y}\hat{y}}^{[1]}-q_3\hat{\phi}_{10,\hat{y}\hat{x}}^{[3]}\right), \tag{83}$$

(c) continuity of effective stress (only $\tau_{\hat{x}\hat{y}}\doteqdot 0$)

$$G\left(2\hat{\phi}_{20,\hat{x}\hat{y}}^{[1]}+\hat{\phi}_{20,\hat{y}\hat{y}}^{[3]}-\hat{\phi}_{20,\hat{x}\hat{x}}^{[3]}\right)=\Psi^2e^{-k_0h}\hat{\xi}_{10,\hat{x}}[2G\left(\hat{\phi}_{10,\hat{x}\hat{x}}^{[1]}+\hat{\phi}_{10,\hat{x}\hat{y}}^{[3]}\right)-\lambda\Lambda^2\hat{\phi}_{10}^{[1]}]-$$

$$G\Psi^2e^{-k_0h}\hat{\xi}_{10}\left(2\hat{\phi}_{10,\hat{x}\hat{y}\hat{y}}^{[1]}+\hat{\phi}_{10,\hat{y}\hat{y}\hat{y}}^{[3]}-\hat{\phi}_{10,\hat{x}\hat{x}\hat{y}}^{[3]}\right); \tag{84}$$

at the porous material/impervious rock interface: $\hat{y}=-k_0B$, $-\infty<\hat{x}<\infty$,

(a) no horizontal displacement for porous material

$$\hat{\phi}_{20,\hat{x}}^{[1]}+\hat{\phi}_{20,\hat{y}}^{[3]}=0, \tag{85}$$

(b) no flux for fluid

$$\alpha_1 \hat{\phi}^{[1]}_{20,\hat{y}} - \alpha_3 \hat{\phi}^{[3]}_{20,\hat{x}} = 0. \tag{86}$$

where $\widetilde{k}_j$ and $\widetilde{\alpha}_j$ (j=1,3) in nonlinear order ε_1^2 are given as (8)-(20) in Huang and Song (1993), and

$$\widetilde{q}_j = 1 - n_0 + \widetilde{\alpha}_j n_0, \quad \text{j=1,3.} \tag{87}$$

Boundary Layer Correction Inside the Boundary Layer

The second longitudinal wave disappears outside the boundary layer but it does exist inside the boundary layer near the water/porous-bed interface, so the complete solution needs to be corrected by further consideration of the second longitudinal wave inside the porous material. Besides, due to the fact that this second longitudinal wave is trapped inside the boundary layer near the water/porous-bed interface, it could not transmit throughout the porous material bed to the interface between the porous material and the impervious rock. In other words, there exists no boundary layer near the porous-material/impervious rock interface due to the deficiency of the second longitudinal wave and where only the first longitudinal wave and the transverse wave exist.

Since a thin boundary layer exists within the porous bed near the water/porous-bed interface, multiple scales are needed to solve the nonlinear boundary value problem for the second longitudinal wave (see Fig. 2). We therefore let $y' = \hat{y}/\varepsilon_2$ to change the scale from $\hat{y}$ to the magnified scale y' in (40b). The difficulty that Chen et al. (1997) encountered, the error due to the first partial derivative based on y of the displacement potential of the second longitudinal wave, is now overcome by proposing two length scales in the vertical direction. After the coordinate transformation of (40b), the boundary value problem of the displacement potential of the second longitudinal wave inside the boundary layer becomes

$O(\varepsilon_1)$

Governing equations

$$\hat{\phi}^{[2]}_{10,\hat{y}'\hat{y}'} + \hat{\phi}^{[2]}_{10} = 0. \tag{88}$$

Boundary conditions: $y' = 0$, $-\infty < \hat{x} < \infty$,

(a) continuity of vertical effective stress (only $\hat{\tau}_{\hat{y}\hat{y}} \fallingdotseq 0$)

$$2G\Lambda^2\hat{\phi}^{[2]}_{1a,\hat{y}\hat{y}'} - \lambda\Lambda^2\hat{\phi}^{[2]}_{10} = \lambda\Lambda^2\hat{\phi}^{[1]}_{10} - 2G\left(\hat{\phi}^{[1]}_{1a,\hat{y}\hat{y}} - \hat{\phi}^{[3]}_{1a,\hat{x}\hat{y}}\right), \tag{89}$$

(b) outside the boundary layer

$$\hat{\phi}^{[2]}_{10} = 0. \tag{90}$$

$O(\varepsilon_1\varepsilon_2)$

Governing equations

$$\hat{\phi}^{[2]}_{11,\hat{y}'\hat{y}'} + \hat{\phi}^{[2]}_{11} = 0. \tag{91}$$

Boundary conditions: $y' = 0$, $-\infty < \hat{x} < \infty$,

(a) continuity of vertical effective stress (only $\tau_{\hat{y}\hat{y}} \fallingdotseq 0$)

$$2G\Lambda^2\hat{\phi}^{[2]}_{1\mathrm{L},\hat{y}\hat{y}'} - \lambda\Lambda^2\hat{\phi}^{[2]}_{11} = \lambda\Lambda^2\hat{\phi}^{[1]}_{11} - 2G\left(\hat{\phi}^{[1]}_{1\mathrm{L},\hat{y}\hat{y}} - \hat{\phi}^{[3]}_{1\mathrm{L},\hat{x}\hat{y}}\right), \tag{92}$$

(b) outside the boundary layer

$$\hat{\phi}^{[2]}_{11} = 0. \tag{93}$$

$O(\varepsilon_1^2)$

Governing equations

$$\hat{\phi}^{[2]}_{20,\hat{y}'\hat{y}'} + \hat{\phi}^{[2]}_{20} = 0. \tag{94}$$

Boundary conditions: $y' = 0$, $-\infty < \hat{x} < \infty$,

(a) continuity of vertical effective stress (only $\tau_{\hat{y}\hat{y}} \fallingdotseq 0$)

$$2G\Lambda^2\hat{\phi}^{[2]}_{20,\hat{y}'\hat{y}'} - \lambda\Lambda^2\hat{\phi}^{[2]}_{20} = -2G\left(\hat{\phi}^{[1]}_{20,\hat{y}\hat{y}} - \hat{\phi}^{[3]}_{20,\hat{x}\hat{y}}\right) + \lambda\Lambda^2\hat{\phi}^{[1]}_{20}$$

$$-\Psi^2\hat{\xi}_{10}e^{-k_0h}\left[2G\left(\hat{\phi}^{[1]}_{10,\hat{y}\hat{y}\hat{y}} + \Lambda^2\hat{\phi}^{[2]}_{11,\hat{y}'\hat{y}'\hat{y}'} - \hat{\phi}^{[3]}_{10,\hat{x}\hat{y}\hat{y}}\right) - \lambda\Lambda^2\left(\hat{\phi}^{[1]}_{10,\hat{y}} + \hat{\phi}^{[2]}_{11,\hat{y}'}\right)\right], \tag{95}$$

(b) outside the boundary layer

$$\hat{\phi}_{20}^{[2]} = 0\,. \tag{96}$$

SOLUTION

After omitting the time factor $e^{-i\omega t}$, the given incoming water wave profile with magnitude a is

$$\eta_{10}(x) = ae^{ik_0x} \qquad (0 < x < \infty). \tag{97}$$

With the input of the incoming water wave, each order of the aforementioned boundary value problem can be solved in sequence. Thus the dimensional solutions of the first longitudinal wave and the transverse wave throughout the entire domain are obtained as follows:

$O(\varepsilon_1)$

$$\phi_{10} = -\frac{i}{k_0}\left[\frac{g}{\omega}\cosh k_0(h-y) - \frac{\omega}{k_0}\sinh k_0(h-y)\right]e^{ik_0x}, \tag{98}$$

$$\phi_{10}^{[1]} = \frac{1}{e^{k_0h}k_0^2}\left(a_{11}e^{K_1k_0y} + a_{12}e^{-K_1k_0y}\right)e^{ik_0x}, \tag{99}$$

$$\phi_{10}^{[3]} = \frac{1}{e^{k_0h}k_0^2}\left(a_{31}e^{K_3k_0y} + a_{32}e^{-K_3k_0y}\right)e^{ik_0x}. \tag{100}$$

$O(\varepsilon_1\varepsilon_2)$

$$\phi_{11} = \frac{\sqrt{gk_0}}{k_0^2}E_5\left[\cosh k_0(h-y) - \frac{\omega^2}{gk_0}\sinh k_0(h-y)\right]e^{ik_0x}, \tag{101}$$

$$\phi_{11}^{[1]} = \frac{1}{e^{k_0h}k_0^2}\left(c_{11}e^{K_1k_0y} + c_{12}e^{-K_1k_0y}\right)e^{ik_0x}, \tag{102}$$

$$\phi_{11}^{[3]} = \frac{1}{e^{k_0h}k_0^2}\left(c_{31}e^{K_3k_0y} + c_{32}e^{-K_3k_0y}\right)e^{ik_0x}, \tag{103}$$

$$\eta_{11} = \frac{i}{k_0}\frac{\omega}{\sqrt{gk_0}}E_5e^{ik_0x}. \tag{104}$$

$O(\varepsilon_1^2)$

$$\phi_{20} = \frac{\sqrt{gk_0}}{k_0^2}\left[E_3 \cosh 2k_0(h-y) + E_4 \sinh 2k_0(h-y)\right]e^{2ik_0x}, \tag{105}$$

$$\phi_{20}^{[1]} = \frac{1}{e^{k_0 h}k_0^2}\left(b_{11}e^{M_1 k_0 y} + b_{12}e^{-M_1 k_0 y}\right)e^{2ik_0x}, \tag{106}$$

$$\phi_{20}^{[3]} = \frac{1}{e^{k_0 h}k_0^2}\left(b_{31}e^{M_3 k_0 y} + b_{32}e^{-M_3 k_0 y}\right)e^{2ik_0x}, \tag{107}$$

$$\eta_{20} = \left(\frac{g}{\omega^2} - \frac{iE_4}{\omega k_0}\sqrt{gk_0}\right)e^{2ik_0x}. \tag{108}$$

The dimensional solutions of the second longitudinal wave obtained by the boundary layer correction approach are:

$O(\varepsilon_1)$

$$\phi_{10}^{[2]} = \frac{1}{e^{k_0 h}k_0^2}\frac{k_1^2}{k_2^2}\left(a_{21}e^{iy'} + a_{22}e^{-iy'}\right)e^{ik_0x}, \tag{109}$$

$O(\varepsilon_1\varepsilon_2)$

$$\phi_{11}^{[2]} = \frac{1}{e^{k_0 h}k_0^2}\frac{k_1^2}{k_2^2}\left(c_{21}e^{iy'} + c_{22}e^{-iy'}\right)e^{ik_0x}, \tag{110}$$

$O(\varepsilon_1^2)$

$$\phi_{20}^{[2]} = \frac{1}{e^{k_0 h}k_0^2}\frac{k_1^2}{k_2^2}\left(b_{21}e^{iy'} + b_{22}e^{-iy'}\right)e^{ik_0x}. \tag{111}$$

Since the solutions of the coefficients such as a_{11}, a_{12}, a_{21}, a_{22}, b_{11}, b_{12}, b_{21}, b_{22}, c_{21}, E_3,..., etc. are in a very long and complicated form, they are omitted herein. However, the solutions could be obtained by mathematical tools, e.g. Mathematica. After solving the displacement potentials, all the other variables can be obtained. The wave profile of the porous bed surface can be found from (20) and (55).

RESULTS AND COMMENTS

Since the second longitudinal wave decays very quickly in the vertical direction inside the boundary layer as shown in Fig. 2, a stretched coordinate is needed to better estimate the partial derivative of the second longitudinal wave. Herein, the present solutions are valid under the constraint of $\| \varepsilon_1 \|^{1/2} > \| \varepsilon_2 \| > \| \varepsilon_1 \|^2$ before liquefaction when referring to Fig. 3.

Table 1 gives the wave condition and the material property of a soft bed. The present results are compared with those of the similar problem with infinite thickness provided by Hsieh et al. (2000) to confirm the validity. The two small parameters $(\| \varepsilon_1 \|, \| \varepsilon_2 \|)$ are found to be (0.052,0.064) which satisfy the constraint $\| \varepsilon_1 \|^{1/2} > \| \varepsilon_2 \| > \| \varepsilon_1 \|^2$. The complex wave number k_0 is found to be (0.103848E+01,0.184387E-06) and thus the wavelength L is 6.05 m.

Fig. 4 shows the distribution of wave-induced pore water pressures under four different thickness. The solid lines denote the present case of finite thick porous bed while the dashed ones denote the case of infinite thick porous bed. These two sets of lines tell that the boundary effect is significant, which feeds pore pressures back into the poroelastic bed very obviously especially when the thickness (B) is less than the half wavelength (L/2). The pore pressures become very large at the top and the bottom of the porous bed in Figs. 4(a) and 4(b). P_0 in Fig. 4 is the wave-induced water pressure on the mean bed surface ($y = 0$), and the nondimensional base B for infinite-thickness case is adopted as the same as in finite-thickness case.

In Fig. 5, the wave-induced horizontal effective stresses of finite-thickness case are larger than those of infinite-thickness case when the thickness is less than the three-fourth wavelength. Besides, this effective stress is influenced obviously by the rigid boundary especially near the top of the porous bed for the case of Fig. 5(a). The vertical effective stresses in Fig. 6 are similar to those of Fig. 5.

In Fig. 7, the shear stresses are affected by the rigid boundary very much when the thickness

is less than the half wavelength. This indicates that the characteristic of shear stresses is totally different from that of normal stresses. In Fig. 8, the wave profiles at porous bed and free surface change very little for different thickness. Fig. 9 shows that the distribution of pore water pressure varies with the depth under different thickness. The locations of occurrence of the wave-induced maximum pore water pressures are also found to be at the top ($y = 0$) or the bottom ($y = -B$) of porous bed depending on the thickness of porous bed. The optimal thickness (B/L) and the maximum pore pressure ($P^{(2)}/P_0$) for the present example are (0.193,1.42) at the surface or (0.145,1.13) at the bottom as shown in Fig. 9. If the maximum pore water pressure is large enough to render the occurrence of zero vertical effective stress by over-loading (e.g. the external force due to earthquake), the porous material is said to be fluidized or liquefied. This surface liquefaction is different from the internal liquefaction of Foda (1987). Although the two sets of contour lines in Fig. 9 are very different in appearance, their values, however, are actually very close when the pore pressures decay under the cases of B/L close to and larger than unity. It is noticeable that for infinite-thickness case the nondimensional base B, which is different from case to case, is chosen as the same one for finite-thickness for each case.

CONCLUSIONS

The conventional Stokes expansion of higher order water waves based on one-parameter $\varepsilon_1 = k_0 a$ is invalid for a soft bed (i.e. $\|\Pi^2\| \fallingdotseq \|k_2^2/k_0^2\| >> 1$) with finite thickness because a boundary layer exists inside the porous bed from the second longitudinal wave. Therefore, the boundary layer correction by adopting a two-parameter perturbation expansion based on $\varepsilon_1 = k_0 a$ and $\varepsilon_2 = k_0/k_2$ is proposed and makes the complicated problem possible to be solved by an analytical method other than by a numerical method. Since the porous material bed in the nature is usually multi-layered, the present study, which makes the complicated

analysis of finite thickness problem possible, is necessary and can be regarded as the first step to further investigations.

The boundary effects of the impervious rock are significant on wave-induced pore water pressure and effective stresses, but very little on wave profiles at the free surface and the porous bed surface. However, the rigid boundary is insignificant to the pore water pressure and effective stresses when the thickness of porous bed is larger than about one wavelength (see Fig. 9). Furthermore, the peak value of pore pressure, which is important in analyzing soil liquefaction, could be found if the wave condition and the porous material are given. For example, the locations of maximum pore pressures in the present study occur at either the top or the bottom of the porous bed depending on the porous material thickness.

ACKNOWLEDGMENT

This study is sponsored by National Science Council of the Republic of China under grants NSC 89-2611-E-002-051.

REFERENCES

Biot, M.A. (1956). "Theory of propagation elastic waves in a fluid saturated porous solid I: Low-frequency range." *JASA*, 28, 168-178.

Chen, T.W., Huang, L.H. and Song, C.H. (1997). "Dynamic response of poroelastic bed to nonlinear water waves." *J. Engrg. Mech., ASCE*, 123, 10, 1041-1049.

Dean R.G. and Dalrymple, R.A. (1991). "*Water wave mechanics for engineers and scientists.*" World Scientific, Singapore.

Deresiewicz, R. and Skalak, R. (1963). "On Uniqueness in Dynamic Poroelasticity." *Bulletin of the Seismological Society of America.* 53(4), 783-788.

Fenton, J.D. (1985). "A fifth-order Stokes theory for steady waves." *Wtrwy., Port, Coast., and Oc. Engrg., ASCE*, 111(2), 216-234.

Foda, M.A. (1987). "Internal dissipative waves in poroelastic media." *Proc. R. Soc. London*, A413, 383-405.

Hsieh, P.C., Huang, L.H. and Wang, T.W. (2000). "Dynamic response of soft poroelastic bed to nonlinear water waves—a boundary layer correction approach," *J. Engrg. Mech., ASCE*, 126(10), 1064-1073.

Huang, L.H. and Chwang, A.T. (1990). "Trapping and absorption of sound waves. II: A sphere covered with a porous layer." *Wave Motion*, 12, 401-414.

Huang, L.H. and Song, C.H. (1993). "Dynamic response of poroelastic bed to water waves." *J. Hydraul. Engrg., ASCE*, 119(9), 1003-1020.

Mei, C. C. (1983). *The Applied Dynamics of Ocean Waves*. John Wiley and Sons, New York.

Moshagen, H. and Torum, A. (1975). "Wave induced pressures in permeable seabeds." *J. Wtrwy. Harb, and Coast. Engrg. Div., ASCE*, 101(1), 49-57.

Putnam, J.A. (1949). "Loss of wave energy due to percolation in a permeable sea-bottom." *Trans. Am. Geophys. Union*, 30, 349-356.

Reid, R. O. and Kajiura, K. (1957). "On the damping of gravity waves over a permeable sea bed." *Trans. Am. Geophys. Union*, 30, 662-666.

Sleath, J.F.A. (1970). "Wave induced pressure in bed of sand." *J. Hydr. Div., ASCE*, 96, 367-378.

Verruijt, A. (1969). Elastic storage of aquifers. *Flow through porous media.* De DeWiest, R. J. M. (Ed.), Academic Press.

TABLE 1. Selection of Wave Condition and Property of a Soft Porous Bed.

Items	Values	Units
Water		
density	1000	kg/m^3
bulk modulus	2.3×10^9	N/m^2
viscosity	0.001	Ns/m^2
depth	2.0	M
wave amplitude	0.05	M
Period	2.0	Sec
Skeleton		
density	2650	kg/m^3
Lame's constant	1.0×10^6	N/m^2
Lame's constant	1.0×10^7	N/m^2
specific permeability	1.0×10^{-12}	m^2
porosity	0.4	

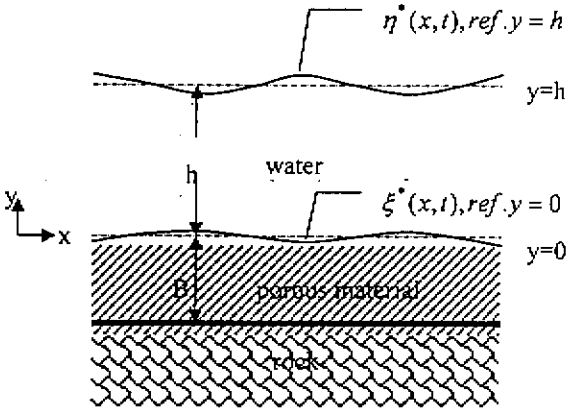

FIG. 1. Definition Sketch.

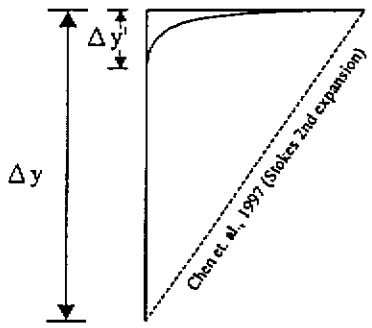

FIG. 2. Schematic Diagram of Vertical Length Scales Inside the Boundary Layer for the Second Longitudinal Wave.

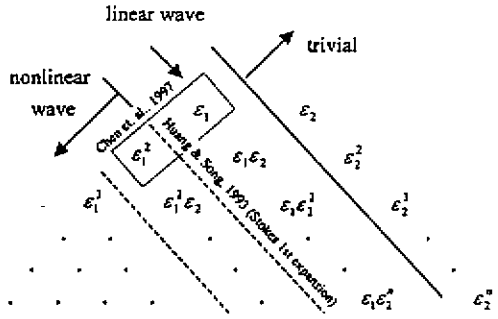

FIG. 3. Schematic Diagram of Two-Parameter Expansion.

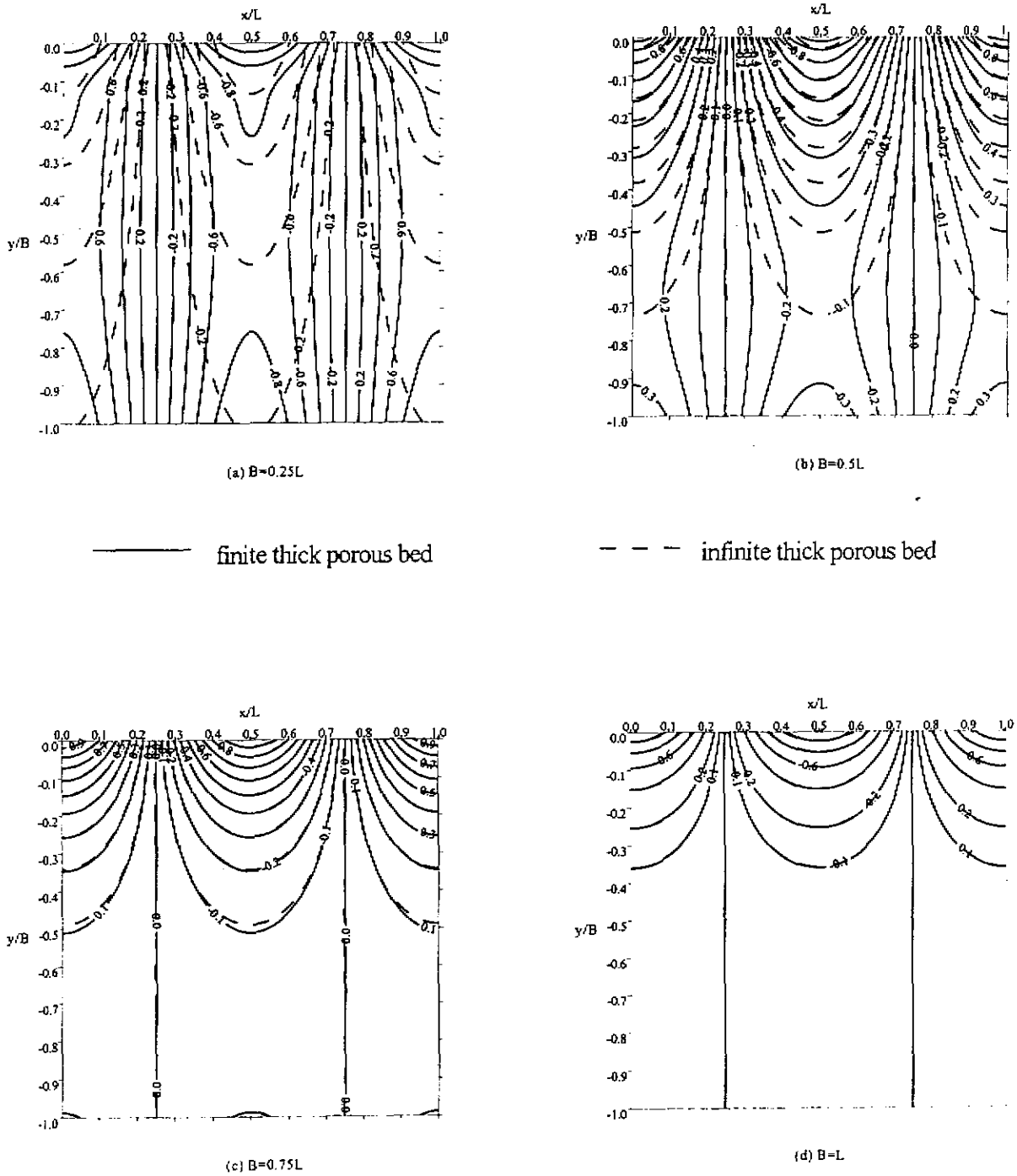

FIG. 4. Distribution of Wave-Induced Pore Water Pressures $|P^{(2)}/P_0|$.

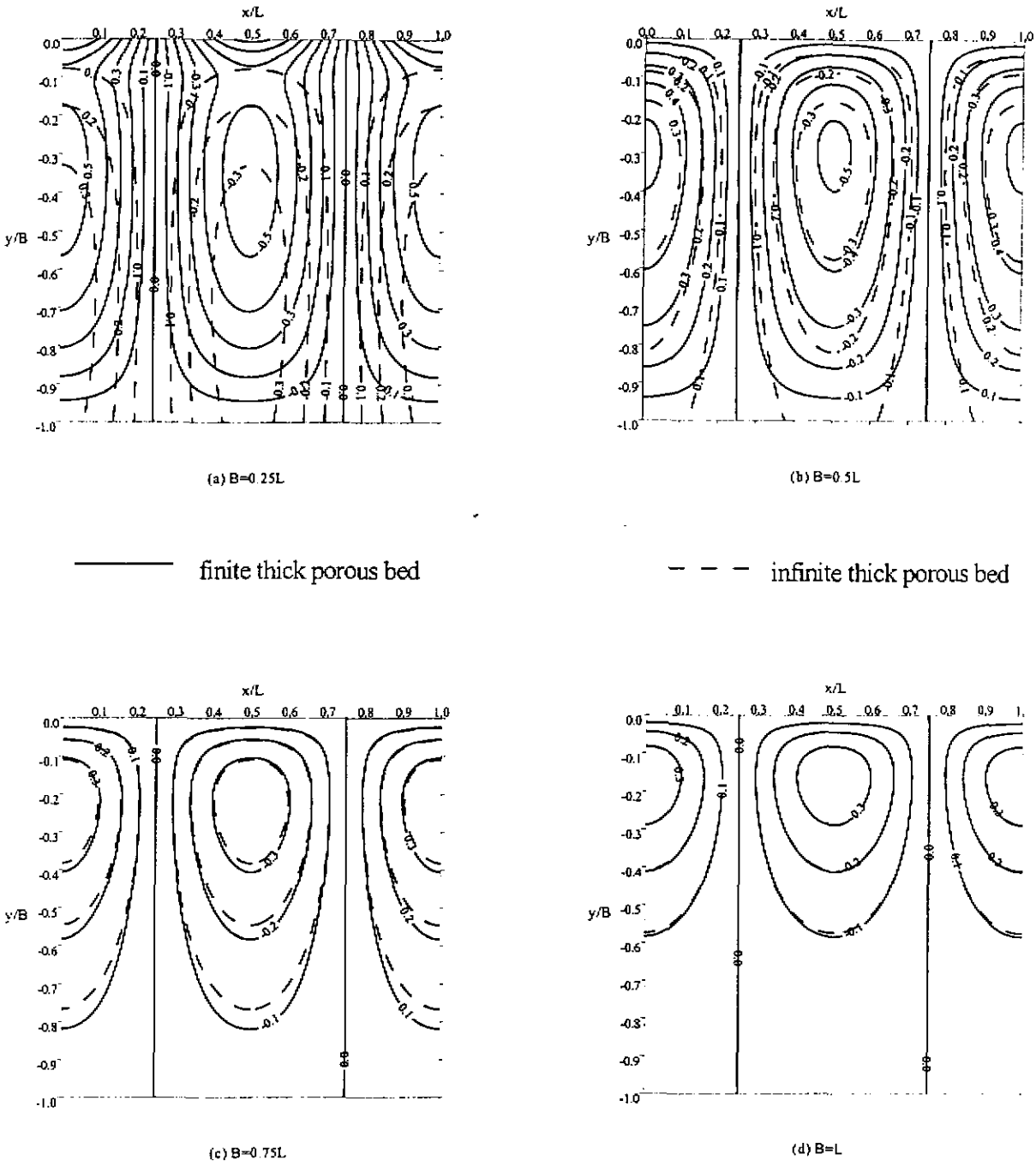

FIG. 5. Distribution of Wave-Induced Horizontal Effective Stresses $|\tau_{xx}/P_0|$.

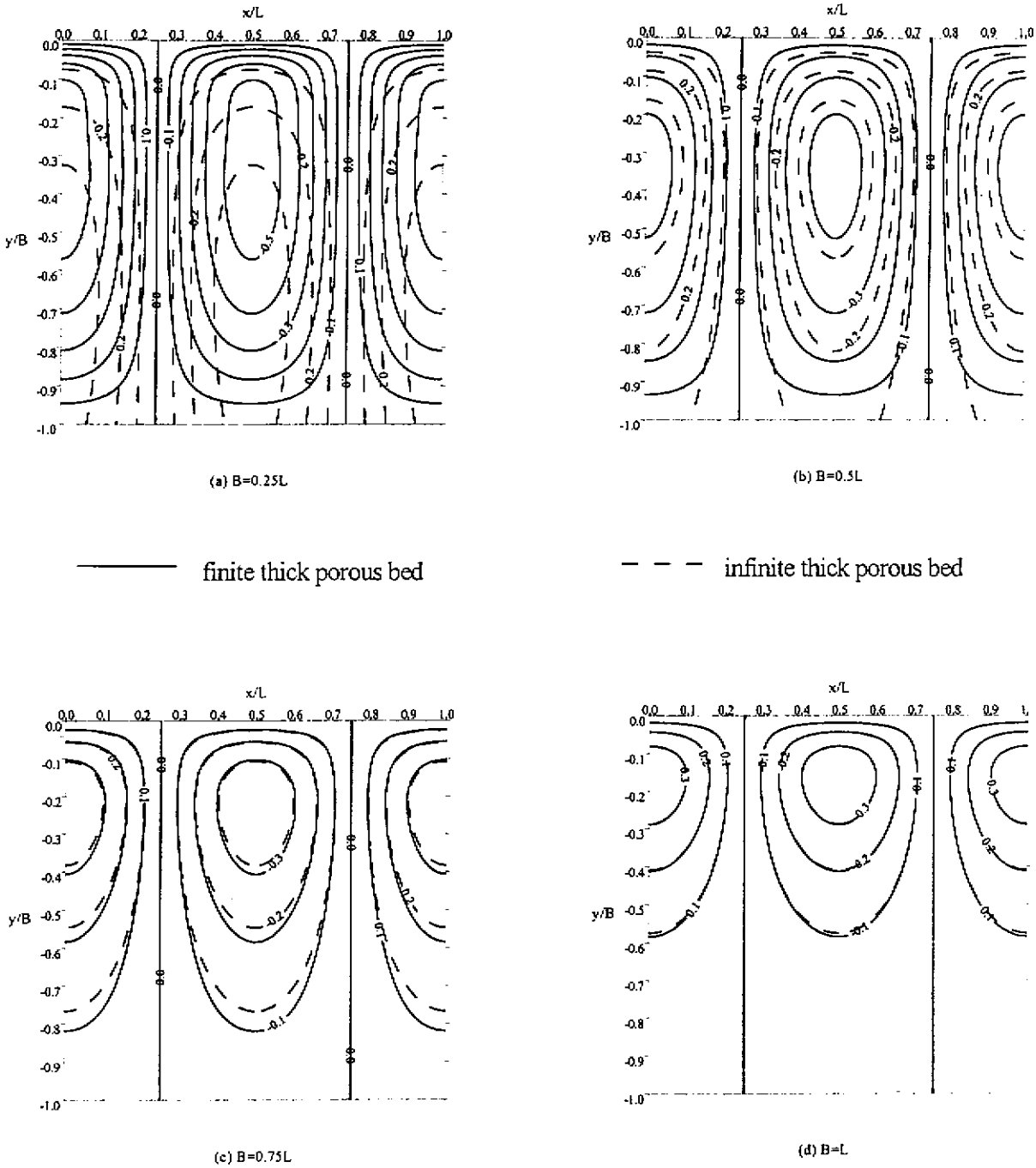

FIG. 6. Distribution of Wave-Induced Vertical Effective Stresses $|\tau_{yy}/P_0|$.

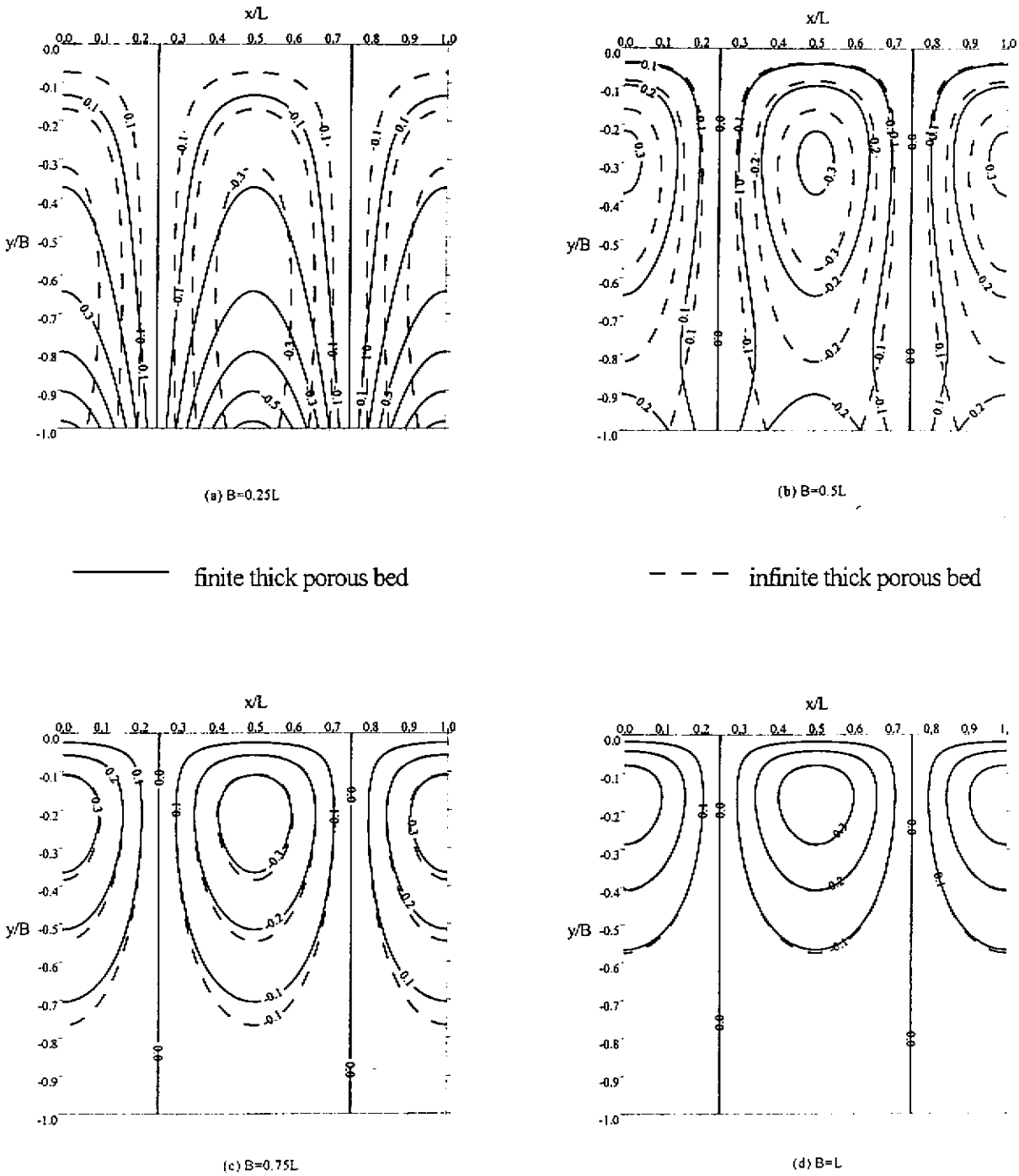

FIG. 7. Distribution of Wave-Induced Shear Stresses $|\tau_{xy}/P_0|$.

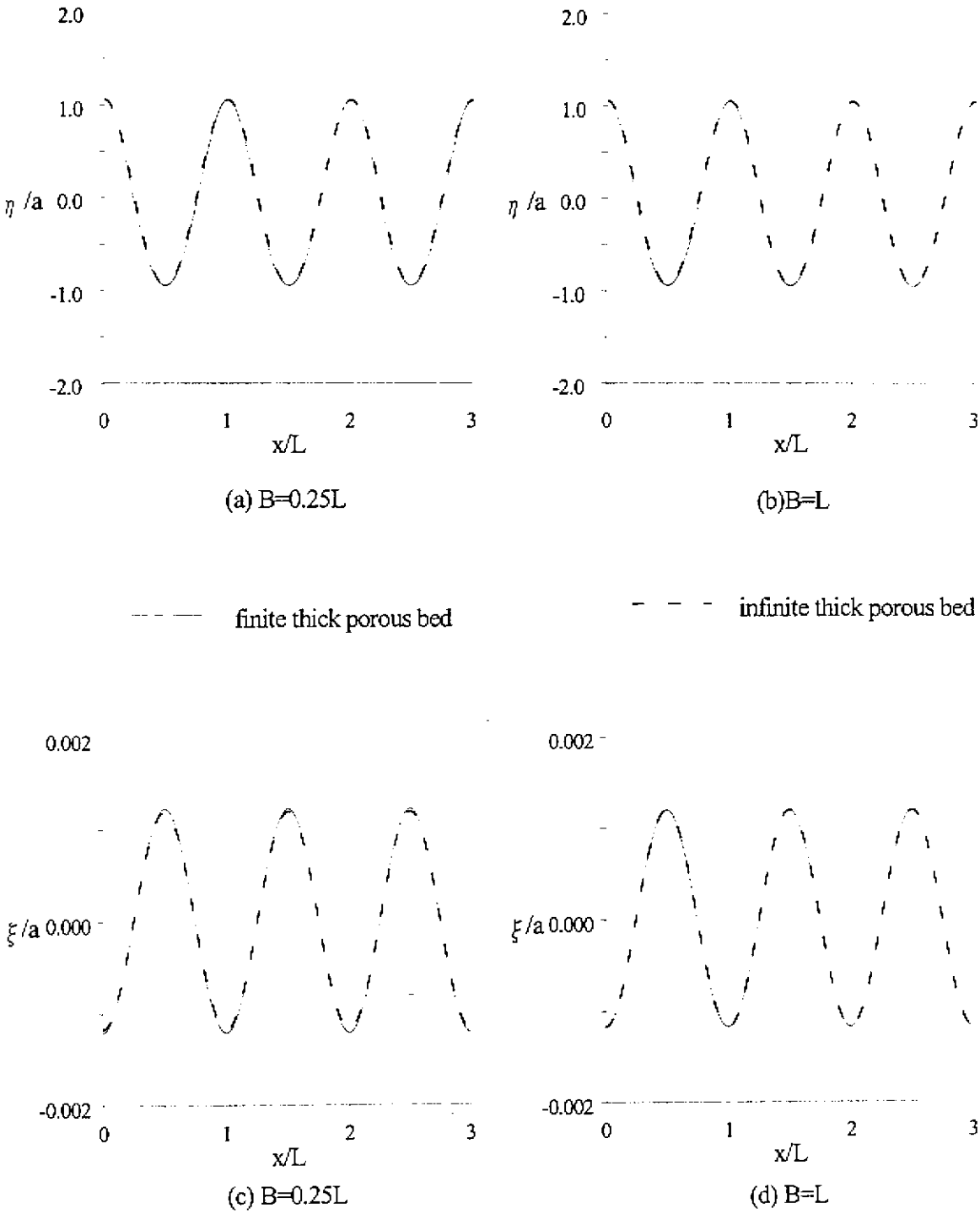

FIG. 8. Wave Profiles of (a)(b)Water and (c)(d)Porous Bed versus Horizontal Distance (Wave Period=2.0 sec).

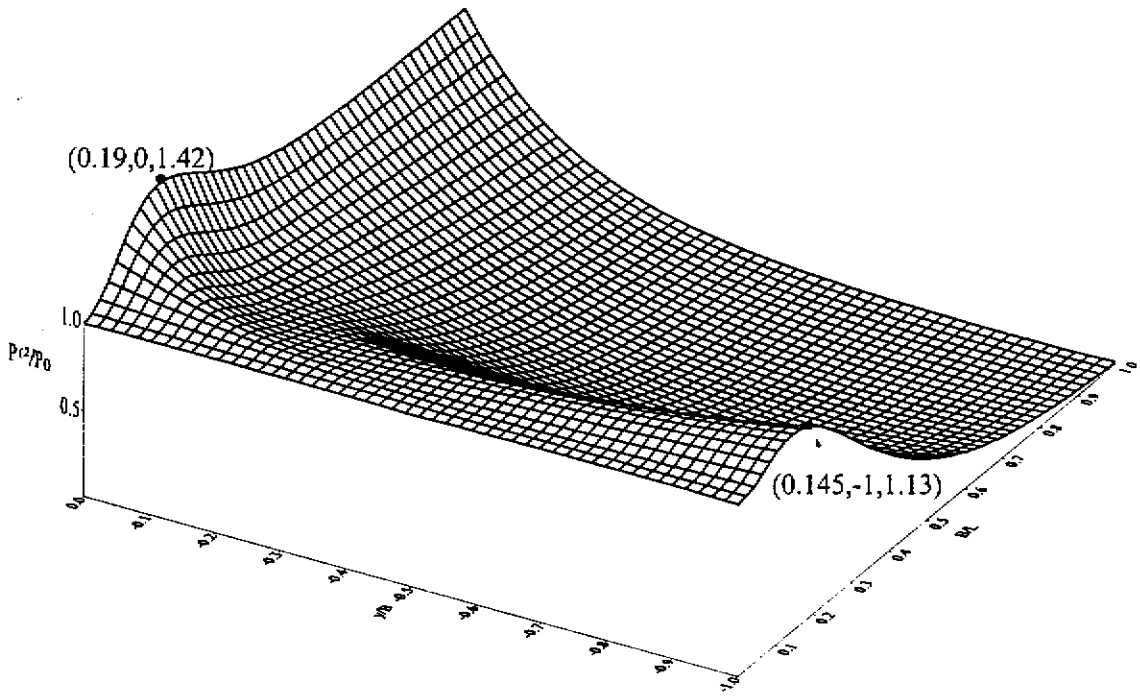

(a)

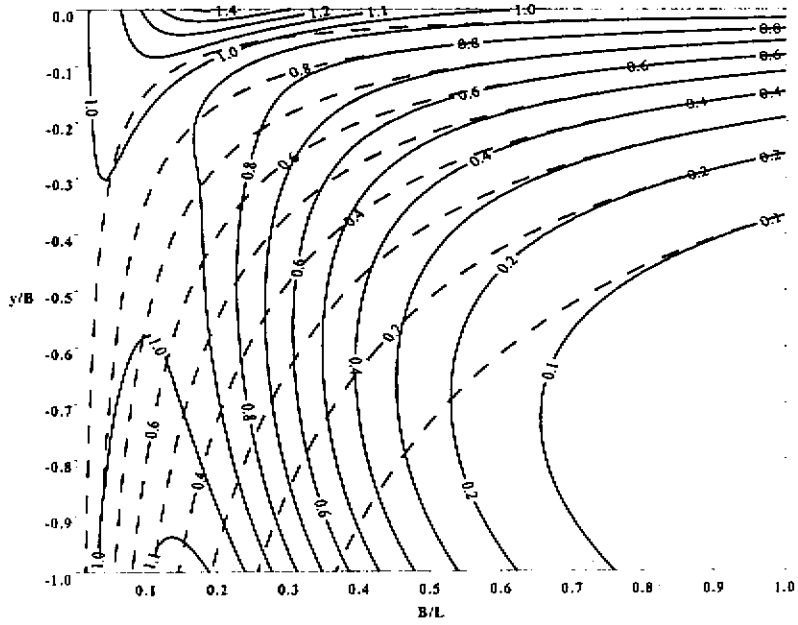

(b)

—— finite thick porous bed — — — infinite thick porous bed

FIG. 9. (a)3D Variation and (b) Contour Lines of Wave-Induced Pore Water Pressures.